Nanoscale

PAPER

View Article Online
View Journal | View Issue

Cite this: *Nanoscale*, 2020, **12**, 12639

Large excitonic effect on van der Waals interaction between two-dimensional semiconductors†

Jiabao Yang, Xiaofei Liu * and Wanlin Guo

Received 17th March 2020,
Accepted 18th May 2020

DOI: 10.1039/d0nr02152k

rsc.li/nanoscale

An exceptionally large excitonic effect on the van der Waals (vdW) interaction between two-dimensional semiconductors is unraveled using the Lifshitz theory in conjunction with the *ab initio* GW plus Bethe–Salpeter equation formalism. Upon consideration of the electron–hole interaction, the vdW energy between two atomistic layers separated by 10 000 angstroms can be larger by a ratio of ~30%, which is an order of magnitude greater than that seen for semi-infinite silicon surfaces. The large influence of the short-range electron–hole interaction on the long-range effect of quantum fluctuations is rooted in the ultra-thin nature of two-dimensional semiconductors which results in not only large exciton binding energy but also amplified roles of low-frequency dielectric responses.

All entities in the vacuum are coupled by the zero-point energy of quantum fluctuations of an electromagnetic field, even if they are electrically neutral. The force felt by the entities, often called the Casimir force or van der Waals (vdW) force, relies on materials' electric and magnetic properties. The dispersion energy per area between parallel semi-infinite surfaces (or finite-thickness plates) of an ideal metal was derived by Casimir to be a power function of distance, $U(d) = -(\pi^2\hbar c)/720d^3$,[1] where $\hbar$ and c are the Planck constant and velocity of light, respectively. For semi-infinite surfaces of a realistic material, the energy–distance relation first given by Lifshitz[2] has one additional scaling constant depending on the material's dielectric and magnetic properties. Another important factor enters into the dispersion interaction is the geometry of the coupled entities. As has long been cognized, the dispersion energies between semi-infinite surfaces, spheres, and cylinders are related to the distance by power functions with different exponents.[3]

The dispersion interaction is particularly important for two-dimensional (2D) materials free from interlayer covalent bonding,[4,5] crucially dominating many of the fundamental processes of 2D materials, including crystallization from atomistic layers into bulk counterparts, fabrication of vdW hetero-structures, dispersion of flakes in solutions, and mechanical coupling with an underlying substrate.[6–12] Generally, 2D materials can be seen as finite-thickness dielectric plates and a plate-like dispersion interaction between them can be anticipated from the Lifshitz theory.[7,13,14] However, unlike macroscopic plates, the geometry and dielectric response of 2D materials are non-trivial. With a thickness of only one atom (*e.g.* graphene and *h*-BN monoatomic layers) or a few atoms (*e.g.* transition-metal dichalcogenide monolayers), they are the thinnest crystalline materials in nature. With the dielectric responses being confined to a 2D or quasi-2D plane,[15] they exhibit novel physical properties associated with electron–electron and electron–phonon interactions.[16,17]

The exceptionally strong Coulomb interaction of electron–hole (e–h) pairs is arguably one of the most remarkable characteristics of 2D materials.[18–20] As illustrated in Fig. 1a, the electric field lines of monopoles can be extended to the vacuum outside a 2D material, making the Coulomb interaction of e–h pairs less effectively screened.[18] As such, the exciton binding energy in 2D semiconductors (or insulators) can be up to a quarter of the bandgap value,[19,20] being far greater than those in typical three-dimensional semiconductors.[21] An ensuing consequence of the strong e–h interaction is the shrinkage of the optical gap relative to the quasiparticle gap and a considerable modulation of the optical absorption spectrum.[22] Since the dispersion interaction is largely determined by materials geometry and dielectric response, several intriguing questions arise: could the long-range dispersion interaction between 2D semiconductors be influenced by the short-range Coulomb interaction of e–h pairs usually with a radius of a few angstroms? If so, to what extent could the dispersion interaction be affected by the excitonic effect? Should the excitonic effect for 2D semiconductors be similar to that for bulk semiconductors?

To answer the questions, we systematically study the excitonic effect on the dispersion interactions of representative 2D

State Key Laboratory of Mechanics and Control of Mechanical Structures, Key Laboratory for Intelligent Nano Materials and Devices of the Ministry of Education, Nanjing University of Aeronautics and Astronautics, 210016 Nanjing, China.
E-mail: liuxiaofei@nuaa.edu.cn

†Electronic supplementary information (ESI) available. See DOI: 10.1039/d0nr02152k

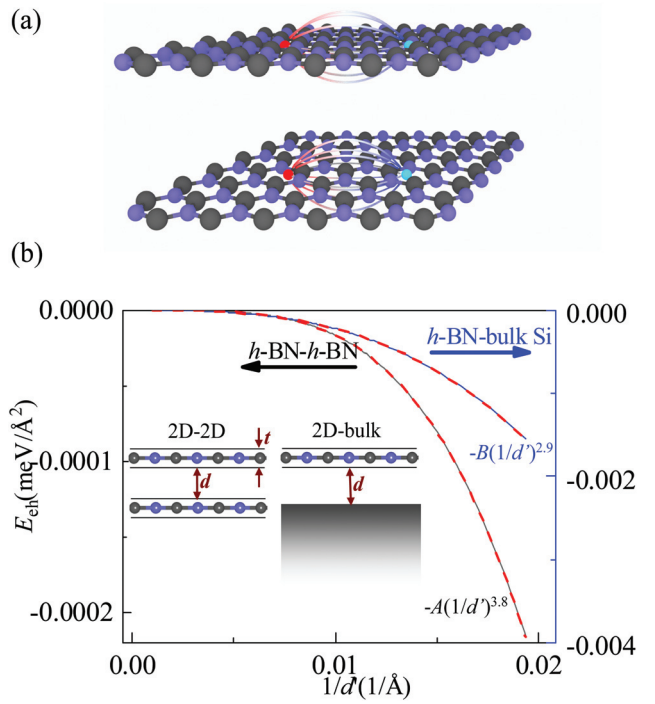

Fig. 1 (a) Schematic illustration of parallel *h*-BN monolayers separated by the vacuum and the e–h interaction in the monolayers. (b) vdW energy per area as a function of inverse distance for the *h*-BN–*h*-BN and *h*-BN–bulk Si systems, calculated with the optical absorption spectra taking into account the e–h interaction. The insets show the models used in calculations. d' is equal to $d + t$ and $d + 0.5t$ for the *h*-BN–*h*-BN and *h*-BN–bulk Si systems, respectively. The $E - 1/d'$ curves in the distance range from 50 to 10 000 Å are fitted by the power functions with an exponent of 3.8 and 2.9, respectively. The Chi-square tolerance for the fitting is set to 1×10^{-9}. The fitted results are visualized with the red dashed curves.

semiconductors, including hexagonal graphene-like monoatomic layers,[23,24] transition-metal dichalcogenide monolayers of 2H phase,[25,26] and functionalized graphene-like materials.[27,28] Our attention is focused on the excitonic effect for parallel 2D semiconductors with an interlayer spacing much shorter than the vdW limit, for which the retardation effect can be neglected and the dispersion interaction is simply the vdW interaction.[29] It is found that the excitonic effect for 2D semiconductors is exceptionally large compared with that for semi-infinite silicon surfaces. Moreover, the modulation of vdW energy between 2D semiconductors by the e–h interaction is distance-dependent, in contrast to the distance-independent effect for semi-infinite surfaces. The mechanisms for both the large excitonic effect and the distance-dependence are rationalized by analyzing the vdW energy contributions from individual Matsubara terms. We also investigate a more experimentally relevant system consisting of an *h*-BN monolayer and a semi-infinite silicon surface, where the excitonic effect is significantly weakened but still much stronger than that for the bulk. Finally, a correlation between the excitonic effect on the long-range vdW energy and that on the static dielectric function is revealed.

In the pioneering work by Hopkins *et al.*, the excitonic effect on the vdW interaction of amorphous silica was studied *via* the Lifshitz theory,[30] with the variation of dielectric response due to the e–h interaction being modeled by an addition of an exciton peak in the one-electron optical spectrum. For a deeper understanding of the excitonic effect on the vdW interaction between 2D semiconductors, we resort to a different strategy, namely the Lifshitz theory in conjunction with the *ab initio* GW plus Bethe–Salpeter equation (BSE) formalism.[31] As will be discussed below, the application of first-principles optical absorption spectra results in distinctive excitonic effects that cannot be captured by the manual addition of an exciton peak. It should also be noted that wave-function-based methods such as the coupled-cluster theory[32] can take into account the excitonic effect on the correlation energy in a fully *ab initio* manner but the computational costs of these methods are unaffordable for the long-range vdW interaction.

The frequency-dependent dielectric functions were calculated using the many-body perturbation theory. First, the mean-filed orbitals and energies were calculated by using density functional theory with local density approximation and norm-conserving pseudopotentials, as implemented in QUANTUM ESPRESSO.[33,34] Second, the quasi-particle energies were computed with the one-shot G0W0 approach using BERKELEYGW.[35] Lastly, the optical absorption spectra taking into account the e–h interaction were calculated by solving the Bethe–Salpeter equation (BSE).[36] To calculate the inverse dielectric matrices, a large number of bands were applied with a specific numbers depending on the material. For example, 656 and 896 bands were used for the *h*-BN and 2H-MoS_2 monolayers, respectively. The applied large band numbers are crucial to the convergence of calculations, since 2D materials are challenging systems for the GW-BSE.[37] With respect to the moment space sampling, coarse and fine grids were adopted for the calculation of inverse dielectric matrices and optical absorption spectra, respectively (*e.g.* $15 \times 15 \times 1$ and $30 \times 30 \times 1$ for *h*-BN). In all calculations, a periodic cell with a thickness of 25 Å was used to avoid any fictitious interaction between neighboring images. Since the output optical absorptance is an average for the monolayer and the surrounding vacuum,[38] the imaginary part of the dielectric function was rescaled by a multiplication coefficient L/t, where L is the thickness of the vacuum slab and t is the effective thickness of the monolayer. In this work, t was set to be the sum of the distance between the top and bottom atomic planes and the diameters of surficial atoms (all assumed to be 1 Å to avoid artifacts varying among materials). We note that the electron–phonon interaction that can broaden the absorption edge[39] and the intrinsic defects of the material that can modify the absorption spectra[40–42] were not considered here owing to the large computational cost.

The Lifshitz formula as introduced in the textbook of Parsegian[3] is applied to evaluate the vdW energies between parallel 2D semiconductors, between an *h*-BN monolayer and a semi-infinite silicon surface, and between parallel semi-infinite silicon surfaces. As illustrated in Fig. 1b, the 2D semi-

conductors are considered as uniform dielectric plates with an effective thickness defined above. The dielectric function along the imaginary frequency axis is obtained from the optical absorption spectrum *via* the Kramers–Kronig (KK) transform,

$$\varepsilon(i\xi) = 1 + \frac{2}{\pi}\int_0^{\infty} \frac{\omega_R \varepsilon''(\omega_R)}{{\omega_R}^2 + \xi^2} d\omega_R,$$

where ε'' is the imaginary part of the dielectric function along the real frequency axis. Taking parallel homogeneous 2D semiconductors separated by a distance of d as an example, the vdW energy per unit area can be expressed as

$$U(d) = \frac{k_B T}{8\pi d^2} {\sum_{N=0}^{\infty}}' \int_{r_N}^{\infty} x \ln[(1 - \overline{\Delta}_{A_m}^{\mathrm{eff}}(\xi_N, x)\overline{\Delta}_{B_m}^{\mathrm{eff}}(\xi_N, x)e^{-x})]dx.$$

Here, k_B is the Boltzmann constant, x is the modulus of the wave vector in the in-plane direction, the temperature T is set to 298 K, the lower limit of the integral r_N is $\frac{2d\sqrt{\varepsilon_m \mu_m}}{c}\xi_N$, and the Matsubara frequencies ξ_N can be $\frac{2\pi k_B T N}{\hbar}$ with N being non-negative integers. The prime on the summation sign means that the contribution from the zero-frequency term is multiplied by 1/2. The reflection coefficient on the plate–vacuum interface in the above equation reads

$$\overline{\Delta}_{im}^{\mathrm{eff}}(t) = \overline{\Delta}_{im} \frac{1 - e^{-x_i(t/d)}}{1 - \overline{\Delta}_{im}^2 e^{-x_i(t/d)}}, \quad i = A, B,$$

where one has $\overline{\Delta}_{im} = \frac{x_m \varepsilon_i - x_i \varepsilon_m}{x_m \varepsilon_i + x_i \varepsilon_m}$, ${x_i}^2 = {x_m}^2 + \left(\frac{2d\xi_N}{c}\right)^2 (\varepsilon_i - \varepsilon_m)$ and $x_m = x$.

Fig. 2a–c show the optical absorption spectra of the *h*-BN, MoS_2 monolayers, and bulk silicon, respectively. Apparently, the e–h interaction induces red-shifts of the lowest absorption peaks in all the materials. For the *h*-BN and MoS_2 monolayers, the absorption edges are shifted from 7.38 to 5.32 eV and from 2.85 to 1.93 eV, respectively, in good accordance with previous reports.[37,43] In the case of silicon, the absorption edge is red-shifted to a much smaller extent of 0.11 eV. These results verify again that the e–h interaction in 2D semiconductors is much stronger than that in typical bulk semiconductors. The repetitious details of the optical absorption spectra for other 2D semiconductors are provided in Fig. S1 of ESI† and will not be discussed, as the large exciton

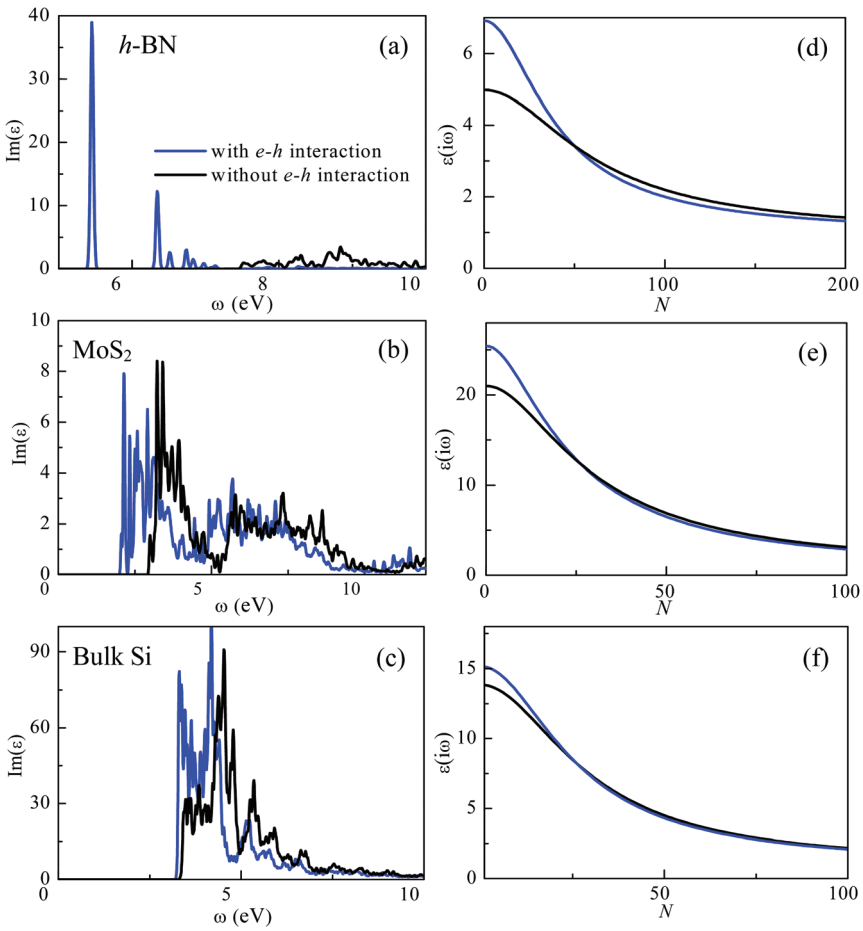

Fig. 2 (a–c) Optical absorption spectra of the *h*-BN, 2H-MoS_2 monolayers, and bulk silicon, calculated both with and without the e–h interaction. (d–f) Dielectric functions as a function of the imaginary Matsubara frequency for the corresponding materials.

binding energy in 2D materials has been a subject of immense research.

Fig. 2e and f present the dielectric function along the imaginary frequency axis that directly enters into the Lifshitz formula. Interestingly, the e–h interaction exerts qualitatively similar effects on the dielectric functions of the *h*-BN, MoS_2 monolayers, and bulk silicon, regardless of the different dimensionalities. As one might expect, the dielectric functions at zero and low frequencies are enhanced by the e–h interaction. Specifically, the ratio of the static dielectric function with the e–h interaction to that without, $\varepsilon_{0\_eh}/\varepsilon_{0\_noeh}$, is 1.39 and 1.21 for the *h*-BN and MoS_2 monolayers, respectively. For silicon, the e–h interaction also induces an appreciable effect with $\varepsilon_{0\_eh}/\varepsilon_{0\_noeh}$ = 1.09, even though the exciton binding energy in silicon is an order of magnitude smaller than that in 2D semiconductors. This is not surprising if one notices that the first absorption peak of silicon is not only moderately red-shifted but also significantly enhanced in amplitude. The enhancement of the static dielectric function can be well rationalized by the KK transformation. At zero or low frequencies, the KK relationship can be approximated as $\varepsilon(i\xi) \approx 1 + \frac{2}{\pi}\int_0^\infty \frac{\varepsilon''(\omega_R)}{\omega_R} d\omega_R$. Then, a red-shift of the absorption peak without change of the profile will certainly increase the dielectric function.

The excitonic effect on the dielectric function turns from positive to negative at higher imaginary frequencies. For briefness of discussion, the critical Matsubara number at which the dielectric function remains unchanged is denoted as N_c. The observed frequency-dependent excitonic effect on the dielectric function can also be rationalized by the KK transformation. With a frequency far exceeding the energy window of optical absorption, the KK relationship can be reduced to $\varepsilon(i\xi) \approx 1 + \frac{2}{\pi}\int_0^\infty \frac{\omega_R \varepsilon''(\omega_R)}{\xi^2} d\omega_R$, indicating a decrease of dielectric function upon a red-shift of the absorption peak without change of the profile. Thus, the increase and decrease of dielectric function at low and high frequencies due to the e–h interaction are a consequence of the causality. It should be mentioned that the addition of an exciton peak in the optical spectrum by Hopkins *et al.* predicted enhanced dielectric responses in the whole imaginary frequency range,[30] deviating from the first-principles results.

We first look into the vdW energy–distance relations in the 2D, 2D-bulk hybrid, and bulk systems. As shown in Fig. 1b, the $E - 1/d'$ curve for parallel *h*-BN monolayers with a distance ranging from 50 to 10 000 Å can be well fitted by a power function, though with a non-integer exponent of 3.8. The slight deviation from the fourth power function of ideal 2D semiconductors (or insulators)[44] could be associated with the finite thickness of realistic materials. For the 2D-bulk hybrid system consisting of *h*-BN and silicon, the fitted power function of the $E - 1/d'$ curve has a non-integer exponent of 2.9, deviating from the third power function of an ideal 2D-bulk hybrid system. On the other hand, the fitted $E - 1/d$ curve for parallel semi-infinite silicon surfaces rigorously obeys a power function with an exponent of 2 (see Fig. S2 of ESI†).

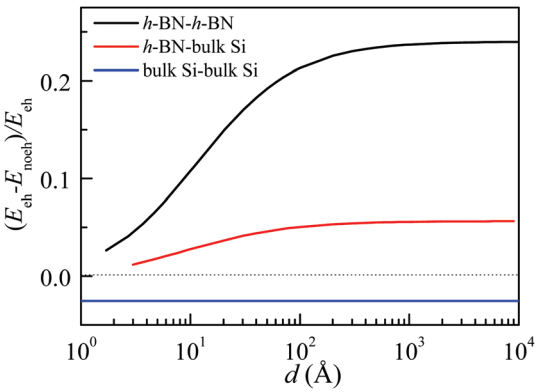

Fig. 3 Effect of the e–h interaction on the vdW interactions between parallel *h*-BN monolayers, between an *h*-BN monolayer and a semi-infinite silicon surface, and between parallel semi-infinite silicon surfaces.

We proceed to examine the excitonic effect on the vdW energy by comparing the ratios $(E_{eh} - E_{noeh})/E_{eh}$ in Fig. 3, where E_{eh} and E_{noeh} are calculated from the dielectric functions with and without the e–h interaction, respectively. For parallel *h*-BN monolayers, E_{eh} is always larger in magnitude than E_{noeh} in the whole considered distance range. At a distance shorter than the near-equilibrium spacing (d = 1.7 Å), $(E_{eh} - E_{noeh})/E_{eh}$ is rather small (2.7%), which could be irrelevant to experimental measurements. The excitonic effect significantly enhances with distance, with $(E_{eh} - E_{noeh})/E_{eh}$ being increased up to 19.2% at d = 50 Å. In the distance range from 50 to 10 000 Å, $(E_{eh} - E_{noeh})/E_{eh}$ increases much moderately, approaching 24.0% at d = 10 000 Å. These results are in good agreement with a previous work by Hobbie *et al.*, where the experimentally measured excitonic peaks are responsible for a 5% enhancement of vdW interaction between semiconducting single-walled carbon nanotubes (SWNTs).[45] Remarkably, the excitonic effect on the long-range vdW interaction between 2D semiconductors is more pronounced than that reported for the SWNTs.

To elucidate the mechanism of the distance-dependent excitonic effect, we depict in Fig. 4a the relative contributions from individual Matsubara terms to the total vdW energy, E_{N_eh}/E_{eh}, as a function of Matsubara frequency. The relative contribution is the highest at the first non-zero Matsubara frequency and then decreases with N. Although the contributions from varying frequencies are uneven, all the Matsubara terms are non-negligible relative to the total vdW energy. For instance, E_{1_eh}/E_{eh} and E_{50_eh}/E_{eh} at d = 4.7 Å are 1.8% and 0.75%, respectively. Notably, the relative contributions vary with distance. As d is increased to 40.7 or 4000.7 Å, E_{1_eh}/E_{eh} is increased to 2.4% or 2.7%, respectively, but E_{50_eh}/E_{eh} is decreased instead. In brief, the role of low-frequency Matsubara terms is amplified in the long-range vdW interaction between 2D semiconductors. A more direct explanation

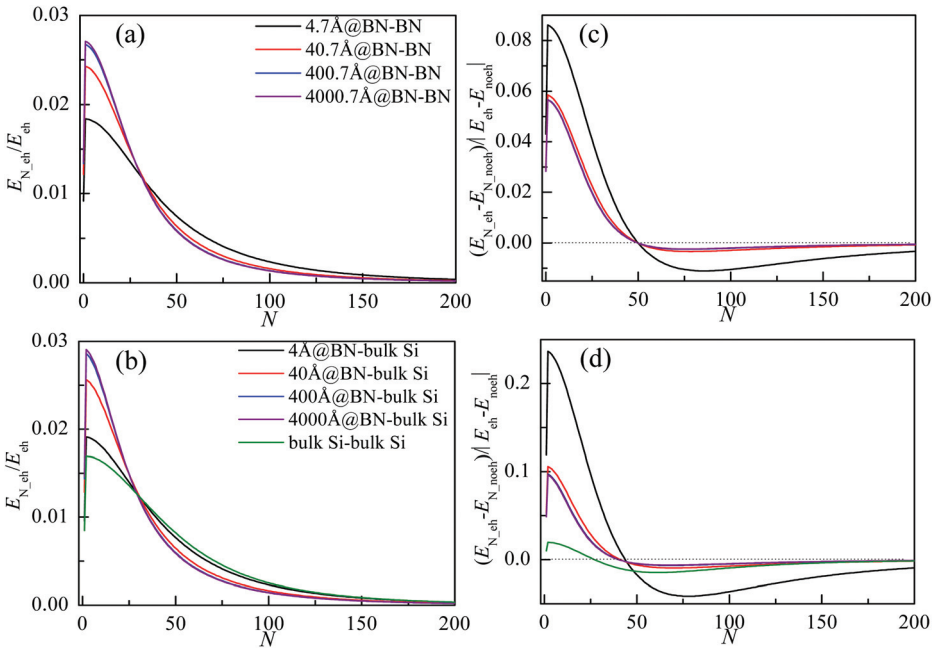

Fig. 4 (a, b) Relative contributions from individual Matsubara terms to the total vdW energy for the *h*-BN–*h*-BN, bulk Si–bulk Si, and *h*-BN–bulk Si systems with varying distances. (c, d) Ratios of the vdW energy differences at individual Matsubara frequencies to the total vdW energy difference.

for the distance-dependence can be obtained by plotting the contribution of the energy difference by individual Matsubara terms to the total vdW energy difference, $(E_{N\_eh} - E_{N\_noeh})/|E_{eh} - E_{noeh}|$. On the ground of intuition, an increased dielectric function will lead to an increased vdW energy and *vice versa*. Indeed, as illustrated in Fig. 4c, the excitonic effects by the Matsubara terms on the two sides of the critical frequency N_c (51 for *h*-BN) are positive and negative, respectively. Since the negative effects from the high-frequency terms diminish with distance, the overall positive effect is enhanced.

The vdW interaction between two silicon semi-infinite surfaces can also be affected by the e–h interaction but to a much smaller extent. As shown in Fig. 3a, $(E_{eh} - E_{noeh})/E_{eh}$ for silicon is distance-independent and estimated to be −2.5%, which is an order of magnitude smaller than that for the long-range interaction between parallel *h*-BN monolayers. Considering the enhanced static dielectric response of silicon due to the e–h interaction, the negative excitonic effect is peculiar. This counterintuitive observation can be understood from the negative effects of Matsubara frequencies higher than the critical frequency (N_c = 28 for silicon). Different from the *h*-BN case where the absolute values of the vdW energy differences $E_{N\_eh} - E_{N\_noeh}$ at the lowest frequencies are much larger than those at frequencies higher than N_c, the negative $E_{60\_eh} - E_{60\_noeh}$ for silicon is comparable in magnitude to the positive $E_{1\_eh} - E_{1\_noeh}$ (Fig. 4d). It should be underscored that neither the overall negative excitonic effect for silicon nor the negative effects of the high-frequency terms for 2D semiconductors could be captured by the manual addition of an exciton peak.

The large excitonic effect for *h*-BN monolayers in comparison with the weak effect for semi-infinite silicon surfaces can be rationalized from two aspects. First, the large exciton binding energy in the 2D semiconductors results in a greater enhancement of low-frequency dielectric response (in terms of percentage). Resultantly, $(E_{N\_eh} - E_{N\_noeh})/(E_{eh} - E_{noeh})$ of low-frequency terms for parallel 2D semiconductors, even with a short distance (*e.g.* 4.7 Å), is higher than that for silicon (Fig. 4c and d). Second, because of the ultra-thin nature of 2D semiconductors, the positive contributions from the low-frequency terms are amplified in the long range, whereas those for silicon are distance-independent.

To see whether the large excitonic effect is universal, we calculate $(E_{eh} - E_{noeh})/E_{eh}$ for 24 representative 2D semiconductors and 4 hetero-bilayers. Despite the distinctive crystal structures, different electronic properties, and varying chemical compositions, the excitonic effect is pronounced in all the 2D materials and five features can be outlined from Fig. 5a–f and Fig. S3 of ESI.† First, the effect is pronounced for the long-range vdW interactions; especially, $(E_{eh} - E_{noeh})/E_{eh}$ for SiC and CrO_2 monolayers can be up to 30% at d = 10 000 Å. Second, the effect in short ranges can be negative for some 2D semiconductors (SiC, GeC, CrO_2, SiF, and SiH). Third, the effect is always positive at larger distances (*e.g.* d > 100 Å). Fourth, the relative modulation of the vdW energy by the e–h interaction can be non-monotonic, *e.g.* for GaS, GaSe and most MX_2. Lastly, hetero-bilayers of 2D semiconductors exhibit similar excitonic effects. The versatility of the excitonic effect is a joint result of all the Matsubara terms, rooted in the non-local connection of the dielectric response with the vdW interaction.[30]

A more experimentally relevant system considered in this study consists of an *h*-BN monolayer suspended above a semi-

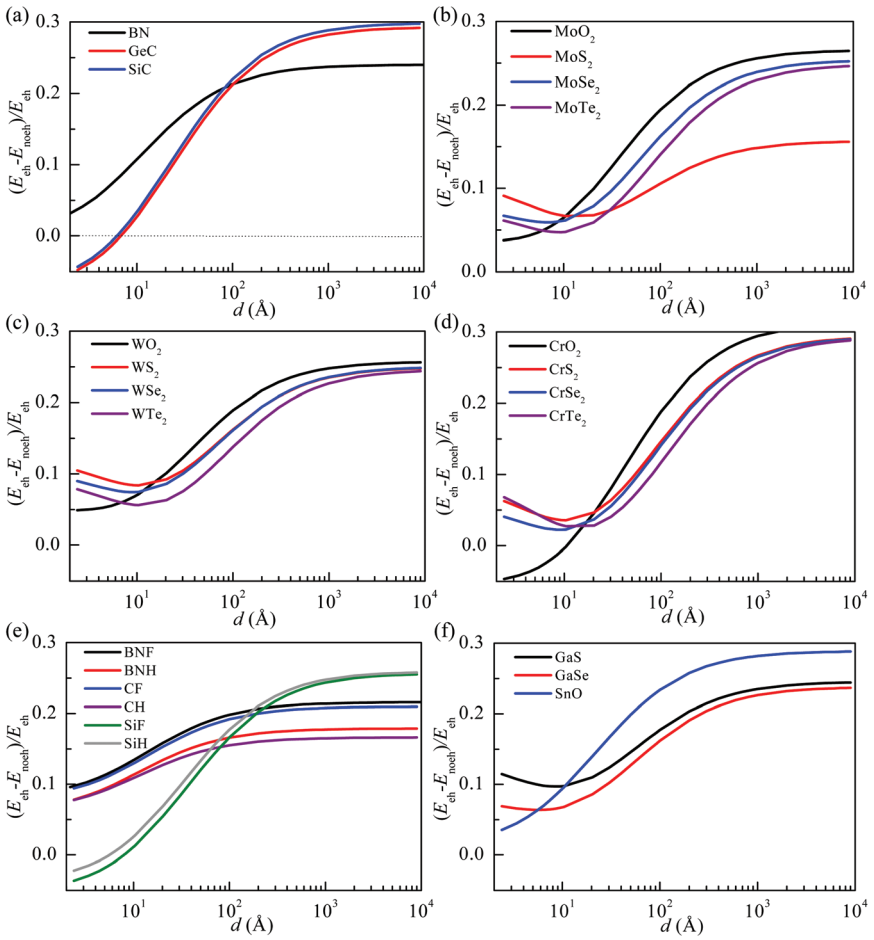

Fig. 5 Effect of the e–h interaction on the vdW energy as a function of distance for representative 2D semiconductors, including (a) hexagonal graphene-like monolayers (*h*-BN, GeC, and SiC), (b, c, d) transition-metal dichalcogenides of 2H phase (MX_2 with M = Mo, W, or Cr and X = O, S, Se, or Te), (e) functionalized graphene-like monolayers (BNF, CF, SiF, BNH, CH, and SiH), and (f) GaS, GaSe, and SnO.

infinite silicon substrate, which is in close relation to mechanical resonators of 2D materials.[46,47] The excitonic effect is significantly weakened in the 2D-bulk hybrid system, with $(E_{eh} - E_{noeh})/E_{eh}$ of 5.6% at d = 10 000 Å (Fig. 3). Based on the above analysis, it can be concluded that the weakened effect is due to the interplay between the positive effect of *h*-BN and negative effect of silicon. Nevertheless, the excitonic effect for the hybrid system is still more pronounced than that for the bulk.

Finally, we seek the correlation between the excitonic effect on the long-range vdW interaction and the fundamental properties of 2D semiconductors. A rather good linear correlation between E_{eh}/E_{noeh} and $\varepsilon_{0\_eh}/\varepsilon_{0\_noeh}$ can be figured out from

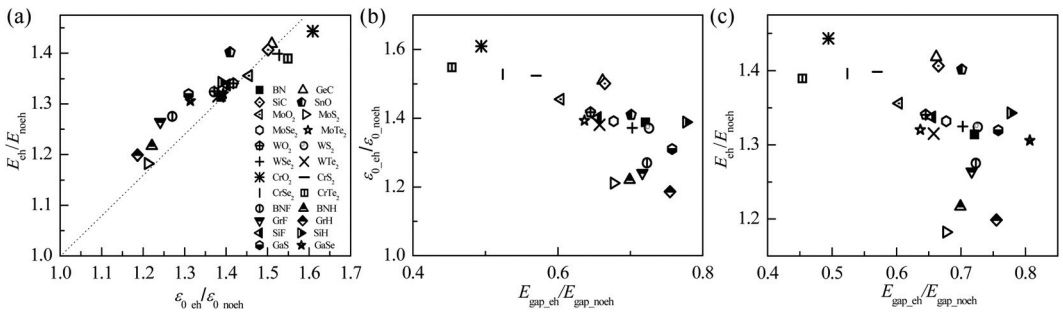

Fig. 6 (a) Correlation of E_{eh}/E_{noeh} at d = 10 000 Å with $\varepsilon_{0\_eh}/\varepsilon_{0\_noeh}$ in the representative 2D semiconductors. ε_0 denotes the static dielectric constant and the sub-label tells whether the e–h interaction is considered. (b) Correlation of $\varepsilon_{0\_eh}/\varepsilon_{0\_noeh}$ with the ratio of absorption edge energies, E_{gap_eh}/E_{gap_noeh}. E_{gap} is the energy level of the absorption edge. (c) Correlation of E_{eh}/E_{noeh} at d = 10 000 Å with E_{gap_eh}/E_{gap_noeh}.

Fig. 6a. Namely, a larger excitonic effect on the static dielectric function is usually associated with a larger effect on the vdW energy. This correlation is straightforward since the low-frequency Matsubara terms are dominant in the long-range vdW interaction. A correlation between $\varepsilon_{0\_eh}/\varepsilon_{0\_noeh}$ and the ratio of absorption edge energies E_{gap_eh}/E_{gap_noeh} can also be observed (Fig. 6b), which is consequential as the polarizability of 2D semiconductors is inversely proportional to the bandgap.[20] The $\varepsilon_{0\_eh}/\varepsilon_{0\_noeh} - E_{gap\_eh}/E_{gap\_noeh}$ relation, however, is much looser, perhaps due to the distinctive crystal structures of considered materials. Despite the two apparent correlations, we cannot figure out a robust link between E_{eh}/E_{noeh} and E_{gap_eh}/E_{gap_noeh} from Fig. 6c.

Whereas the importance of vdW interaction in 2D materials with near-equilibrium interlayer distances has been extensively studied and well recognized,[48,49] the practical meaning of the vdW interaction in 2D materials with large distances is largely overlooked. To clarify this point, we evaluate the vdW pressure exerted on the *h*-BN monolayer in the *h*-BN–*h*-BN and *h*-BN–bulk Si systems, both with a distance of 50 Å. The vdW pressure in the *h*-BN–*h*-BN system is estimated to be 0.17 times the barometric pressure (atm), while that in the *h*-BN–bulk Si system is 1.1 atm. Thus, the long-range vdW interaction and the revealed excitonic effect indeed have an influence on the physical and mechanical performances of these systems. For instance, the mechanical deformation of a 2D monolayer should be determined jointly by the vdW pressure and the gas pressure when it is supported by a perforated substrate and used as a molecule sieve.[50,51]

In conclusion, we have systematically investigated the excitonic effect on the van der Waals interaction between 2D semiconductors by using the Lifshitz theory in conjunction with the GW plus Bethe–Salpeter equation formalism. The excitonic effect for 2D semiconductors is found to be exceptionally large, being an order of magnitude greater than that for bulk silicon, owing to the ultra-thin nature that leads to not only large exciton binding energy but also amplified roles of low-frequency dielectric responses. These findings shed new light on the coupling between the short-range electron–hole interaction and long range-effect of quantum fluctuations and should be instrumental in the design of low-dimensional electro-mechanical devices.

Conflicts of interest

There are no conflicts to declare.

Acknowledgements

This work was supported by the National Natural Science Foundation of China (11702132 and 51535005) and the National Key Research and Development Program of China (2019YFA0705400). X. L. is grateful to the support from China Postdoctoral Science Foundation (No. 2016M600408 and 2017T100362) and the Natural Science Foundation of Jiangsu Province (No. BK20170770).

References

1 H. B. G. Casimir and D. Polder, *Phys. Rev.*, 1948, **73**, 360–372.
2 E. M. Lifshitz, *Sov. Phys. JETP*, 1956, **2**, 73–83.
3 V. A. Parsegian, *van der Waals forces: a handbook for biologists, chemists, engineers, and physicists*, Cambridge University Press, 2005.
4 K. S. Novoselov, A. K. Geim, S. V. Morozov, D. Jiang, Y. Zhang, S. V. Dubonos, I. V. Grigorieva and A. A. Firsov, *Science*, 2004, **306**, 666–669.
5 Y.-M. Lin, C. Dimitrakopoulos, K. A. Jenkins, D. B. Farmer, H.-Y. Chiu, A. Grill and P. Avouris, *Science*, 2010, **327**, 662–662.
6 L. A. Girifalco and M. Hodak, *Phys. Rev. B: Condens. Matter Mater. Phys.*, 2002, **65**, 125404.
7 B. Li, J. Yin, X. Liu, H. Wu, J. Li, X. Li and W. Guo, *Nat. Nanotechnol.*, 2019, **14**, 567–572.
8 J. N. Coleman, M. Lotya, A. O'Neill, S. D. Bergin, P. J. King, U. Khan, K. Young, A. Gaucher, S. De, R. J. Smith, I. V. Shvets, S. K. Arora, G. Stanton, H. Y. Kim, K. Lee, G. T. Kim, G. S. Duesberg, T. Hallam, J. J. Boland, J. J. Wang, J. F. Donegan, J. C. Grunlan, G. Moriarty, A. Shmeliov, R. J. Nicholls, J. M. Perkins, E. M. Grieveson, K. Theuwissen, D. W. McComb, P. D. Nellist and V. Nicolosi, *Science*, 2011, **331**, 568–571.
9 N. Inui, *J. Appl. Phys.*, 2016, **119**, 104502.
10 M. Aykol, B. Hou, R. Dhall, S. W. Chang, W. Branham, J. Qiu and S. B. Cronin, *Nano Lett.*, 2014, **14**, 2426–2430.
11 L. Kou, B. Yan, F. Hu, S.-C. Wu, T. O. Wehling, C. Felser, C. Chen and T. Frauenheim, *Nano Lett.*, 2013, **13**, 6251–6255.
12 L. Kou, S.-C. Wu, C. Felser, T. Frauenheim, C. Chen and B. Yan, *ACS Nano*, 2014, **10**, 10448–10454.
13 M. Bordag, G. Klimchitskaya and V. Mostepanenko, *Phys. Rev. B: Condens. Matter Mater. Phys.*, 2012, **86**, 165429.
14 G. Klimchitskaya and V. Mostepanenko, *Phys. Rev. B: Condens. Matter Mater. Phys.*, 2013, **87**, 075439.
15 P. Cudazzo, I. V. Tokatly and A. Rubio, *Phys. Rev. B: Condens. Matter Mater. Phys.*, 2011, **84**, 085406.
16 P. Cudazzo, C. Attaccalite, I. V. Tokatly and A. Rubio, *Phys. Rev. Lett.*, 2010, **104**, 226804.
17 T. Sohier, M. Gibertini, M. Calandra, F. Mauri and N. Marzari, *Nano Lett.*, 2017, **17**, 3758–3763.
18 A. Chernikov, T. C. Berkelbach, H. M. Hill, A. Rigosi, Y. Li, O. B. Aslan, D. R. Reichman, M. S. Hybertsen and T. F. Heinz, *Phys. Rev. Lett.*, 2014, **113**, 076802.
19 J. H. Choi, P. Cui, H. Lan and Z. Zhang, *Phys. Rev. Lett.*, 2015, **115**, 066403.
20 Z. Jiang, Z. Liu, Y. Li and W. Duan, *Phys. Rev. Lett.*, 2017, **118**, 266401.

21 B. D. Malone, S. G. Louie and M. L. Cohen, *Phys. Rev. B: Condens. Matter Mater. Phys.*, 2010, **81**, 115201.
22 X. Liu and W. Guo, *Phys. Rev. B*, 2019, **99**, 035401.
23 Y. Kobayashi, K. Kumakura, T. Akasaka and T. Makimoto, *Nature*, 2012, **484**, 223–227.
24 H. Şahin, S. Cahangirov, M. Topsakal, E. Bekaroglu, E. Akturk, R. T. Senger and S. Ciraci, *Phys. Rev. B: Condens. Matter Mater. Phys.*, 2009, **80**, 155453.
25 B. Radisavljevic, A. Radenovic, J. Brivio, V. Giacometti and A. Kis, *Nat. Nanotechnol.*, 2011, **6**, 147–150.
26 L. F. Mattheiss, *Phys. Rev. B: Solid State*, 1973, **8**, 3719–3740.
27 K.-J. Jeon, Z. Lee, E. Pollak, L. Moreschini, A. Bostwick, C.-M. Park, R. Mendelsberg, V. Radmilovic, R. Kostecki and T. J. Richardson, *ACS Nano*, 2011, **5**, 1042–1046.
28 X. Liu, J. Yang and W. Guo, *Phys. Rev. B*, 2020, **101**, 045428.
29 F. Capasso, J. N. Munday, D. Iannuzzi and H. B. Chan, *IEEE J. Quantum Electron.*, 2007, **13**, 400–414.
30 J. C. Hopkins, D. M. Dryden, W.-Y. Ching, R. H. French, V. A. Parsegian and R. Podgornik, *J. Colloid Interface Sci.*, 2014, **417**, 278–284.
31 B. C. Shih, Y. Xue, P. Zhang, M. L. Cohen and S. G. Louie, *Phys. Rev. Lett.*, 2010, **105**, 146401.
32 R. J. Bartlett and M. Musiał, *Rev. Mod. Phys.*, 2007, **79**, 291–352.
33 P. Giannozzi, S. Baroni, N. Bonini, M. Calandra, R. Car, C. Cavazzoni, D. Ceresoli, G. L. Chiarotti, M. Cococcioni and I. Dabo, *J. Phys.: Condens. Matter*, 2009, **21**, 395502.
34 P. Hohenberg and W. Kohn, *Phys. Rev.*, 1964, **136**, B864–B871.
35 J. Deslippe, G. Samsonidze, D. A. Strubbe, M. Jain, M. L. Cohen and S. G. Louie, *Comput. Phys. Commun.*, 2012, **183**, 1269–1289.
36 M. Rohlfing and S. G. Louie, *Phys. Rev. B: Condens. Matter Mater. Phys.*, 2000, **62**, 4927.
37 D. Y. Qiu, H. Felipe and S. G. Louie, *Phys. Rev. Lett.*, 2013, **111**, 216805.
38 X. Liu, Z. Zhang and W. Guo, *Phys. Rev. B*, 2018, **97**, 241411.
39 J. Noffsinger, E. Kioupakis, C. G. Van de Walle, S. G. Louie and M. L. Cohen, *Phys. Rev. Lett.*, 2012, **108**, 167402.
40 S. Tongay, J. Suh, C. Ataca, W. Fan, A. Luce, J. S. Kang, J. Liu, C. Ko, R. Raghunathanan, J. Zhou, F. Ogletree, J. Li, J. C. Grossman and J. Wu, *Sci. Rep.*, 2013, **3**, 2657.
41 D. Edelberg, D. Rhodes, A. Kerelsky, B. Kim, J. Wang, A. Zangiabadi, C. Kim, A. Abhinandan, J. Ardelean, M. Scully, D. Scullion, L. Embon, R. Zu, E. J. G. Santos, L. Balicas, C. Marianetti, K. Barmak, X. Zhu, J. Hone and A. N. Pasupathy, *Nano Lett.*, 2019, **19**, 4371–4379.
42 W. Wang, H. Shu, J. Wang, Y. Cheng, P. Liang and X. Chen, *ACS Appl. Mater. Interfaces*, 2020, **12**, 9563–9571.
43 L. Wirtz, A. Marini and A. Rubio, *Phys. Rev. Lett.*, 2006, **96**, 126104.
44 J. F. Dobson, A. White and A. Rubio, *Phys. Rev. Lett.*, 2006, **96**, 073201.
45 E. K. Hobbie, T. Ihle, J. M. Harris and M. R. Semler, *Phys. Rev. B: Condens. Matter Mater. Phys.*, 2012, **85**, 245439.
46 C. Chen, S. Rosenblatt, K. I. Bolotin, W. Kalb, P. Kim, I. Kymissis, H. L. Stormer, T. F. Heinz and J. Hone, *Nat. Nanotechnol.*, 2009, **4**, 861–867.
47 J. A. Weldon, B. Aleman, A. Sussman, W. Gannett and A. K. Zettl, *Nano Lett.*, 2010, **10**, 1728–1733.
48 W. Gao and A. Tkatchenko, *Phys. Rev. Lett.*, 2015, **114**, 096101.
49 T. Björkman, A. Gulans, A. Krasheninnikov and R. Nieminen, *J. Phys.: Condens. Matter*, 2012, **24**, 424218.
50 S. P. Koenig, L. Wang, J. Pellegrino and J. S. Bunch, *Nat. Nanotechnol.*, 2012, **7**, 728–732.
51 M. Lozada-Hidalgo, S. Hu, O. Marshall, A. Mishchenko, A. Grigorenko, R. Dryfe, B. Radha, I. Grigorieva and A. Geim, *Science*, 2016, **351**, 68–70.